Effect of heat treatment on the migration behaviour of selenium implanted into polycrystalline SiC

ZAY Abdalla[1,*], MYA Ismail[1], EG Njoroge[1], E Wendler[2], JB Malherbe[1], TT Hlatshwayo[1]

[1]*Department of Physics, University of Pretoria, Pretoria 0002, South Africa*

[2]*Institut für Festkörperphysik, Friedrich-Schiller Universität Jena, 07743 Jena, Germany*

ABSTRACT

This study reviews the migration behaviour of selenium in polycrystalline SiC, which acts as the main diffusion barrier in the coated fuel particles for Very High Temperature Reactors. Se ions of 200 keV were implanted into polycrystalline SiC wafers to a fluence of 1×10^{16} cm^{-2} at three temperatures, which were room temperature, 350 °C and 600 °C. The implanted samples were annealed at temperatures ranging from 1000 to 1500 °C in steps of 100 °C for 10 hours. The migration of implanted Se was monitored by Rutherford backscattering spectrometry (RBS) while structural and morphological changes were monitored by Raman spectroscopy and scanning electron microscopy (SEM). Implantation of Se at room temperature amorphized the near surface region of the SiC substrates, while in samples implanted above the critical amorphization temperature the crystal structure was retained with some radiation damage. Annealing at 1000°C resulted in the recrystallization of the amorphized SiC layer. In the case of room temperature implantation, the broadening of the implanted Se profile in RBS spectra was observed to occur after annealing at 1300°C and became significant with an increase in annealing temperature. This broadening was accompanied by a peak shift towards the surface and loss of implanted Se. No broadening was observed in samples implanted above the critical amorphization temperature, but the peak shift towards the surface began after annealing at 1300 °C in samples implanted at 350 °C and 600 °C.

Keywords: Ion implantation; Polycrystalline SiC; Recrystallization; Diffusion

1. INTRODUCTION

The Pebble Bed Modular Reactor (PBMR) is a type of Very High Temperature Gas Cooled Reactor (VHTGR), which uses fuel in the form of tristructural isotropic (TRISO)-coated particles [1][2]. This particle is composed of a fuel kernel (UO_2), a low-density carbon buffer layer, an inner pyrolytic carbon (IPyC) layer, a silicon carbide (SiC) layer, and the outer pyrolytic carbon (OPyC) layer [3][4]. The success of the PBMR is highly dependent on the performance of the TRISO particles and the quality of its components [4]. The function of these layers is to retain the radioactive fission products within the fuel particles under normal operation and even under accident conditions [5] [6]. Based on the outstanding properties of silicon carbide as reported in [7], the SiC layer is considered to be the most important structure in the TRISO fuel particles [8]. It must also be able to withstand high temperatures. The outlet temperature of some of the VHTGRs is about 900°C [2]. Moreover, the temperature inside the TRISO fuel particles is higher than the outlet temperature [5].

Selenium (Se) is a non-metallic element, which have many radioactive and stable isotopes. Se The radioactive isotope, ^{79}Se, is present in the nuclear fission products of uranium [9]. The radiological hazard of selenium comes from the emitted beta particle during its radioactive decay, which is associated with an increased likelihood of cancer [9]. To the best of our knowledge, not much has been done on the migration of Se in SiC. Only the migration of Se implanted into polycrystalline SiC has been investigated at temperatures ≥ 1000 °C [10]. To get more insight in the migration of this fission product, the effect of radiation damage in the migration of Se need to be investigated. The purpose of this study is to investigate the effect of heat treatment at temperatures ≥1000 °C on the migration behaviour of Selenium (Se) implanted into polycrystalline SiC at 350 and 600 °C. The findings of this study are compared with our recently published results of Se implanted into polycrystalline SiC at RT to obtain the more insight in the influence of radiation damage in the migration of Se in SiC.

2. EXPERIMENTAL PROCEDURE

Polycrystalline SiC wafers from Valley Design Corporation were used in this investigation. The as received SiC consisted of mainly columnar crystallites aligned along the growth direction with

diameters of a few micrometers [11]. Some smaller crystals not parallel to the columns were also present. These wafers were composed of mainly 3C-SiC with some traces of 6H-SiC.

^{80}Se ions with an energy of 200 keV were implanted into SiC to a fluence of 1×10^{16} cm^{-2}. The flux was kept below 10^{13} cm^{-2}s^{-1} to minimize radiation induced heating. Implantations were performed at room temperature, 350 °C and 600 °C under vacuum. Si or C atoms sputtering does not occur in the used implantation conditions. The implantation was performed at the Friedrich-Schiller-University Jena, Germany. Some of the implanted samples were isochronal annealed in vacuum using a computer controlled Webb 77 graphite furnace at temperatures ranging from 1000 to 1500°C in steps of 100°C for 10 hours. The distribution of the implanted Se were monitored after each annealing step using Rutherford backscattering spectroscopy (RBS) with a collimated beam of He^+ particles of 1.6 MeV, the silicon (Si) surface barrier detector at a scattering angle of 165° was used to detect the backscattered particles.

The beam current was approximately 15 nA and 24 μC was collected per measurement. The RBS spectra in energy in channel number were converted into depth in nm using ZBL stopping powers [12], and density of pristine SiC (3.21 g cm^{-3}). The Se depth profiles were fitted to a Gaussian function to extract the projected ranges (Rp) and range stragglings (ΔRp) [13]. The morphologies of the surfaces before and after annealing were investigated by a Zeiss Ultra 55 field emission gun scanning electron microscopy (FEG-SEM) with an in-lens detector. An accelerating voltage of 2 kV was used. The microstructural changes in SiC due to the implantation and annealing were monitored by using a Jobin Yvon, Horiba$^{(C)}$ TX64000 triple Raman spectrometer. The investigations were performed in the visible region with a 514.5 nm of Ar/Kr laser lines as exciting radiation. The spot of ~2μm^2 was used to focus the laser beam and collected by a 50X objective

3. RESULTS AND DISCUSSION

In Fig. 1, the RBS depth profiles of samples implanted at room temperature 350 °C and 600 °C, the SRIM simulated Se profile and SRIM simulated dpa (damage in displacement per atom) using the full-cascades setting are shown. In the SRIM calculations, we assumed the threshold displacement energy of Si and C atoms to be 35 and 20 eV, respectively [14]. The depth profiles of as-implanted samples obtained from RBS were fitted to Edgeworth distribution equation to extract the first four moments. The agreement between the projected ranges, together with their

ranges straggling is within the profile fitting errors for Gaussian distribution and experimental error of the RBS measurements – see Table.1. The average of the projected range of 89.5 ± 2.9 nm is very comparable to the theoretical value of 89.6 ± 2.9 nm. The results showed that the difference of the range straggling between the average of experimental measurements (33 ± 2.9 nm) and theoretical value (26.5 ± 2.9 nm) is higher than that of the projected range. This discrepancy in the straggling can be attributed to the fact that the radiation enhanced diffusion in implantation process and the gurgitation of state density of charge as ions penetrate target are not considered in SRIM calculations [15]. Also shown in Table.1 the kurtosis (β) and skewness (γ) values obtained from the RBS as implanted samples and SRIM calculation indicate that the profiles are nearly Gaussian distribution.

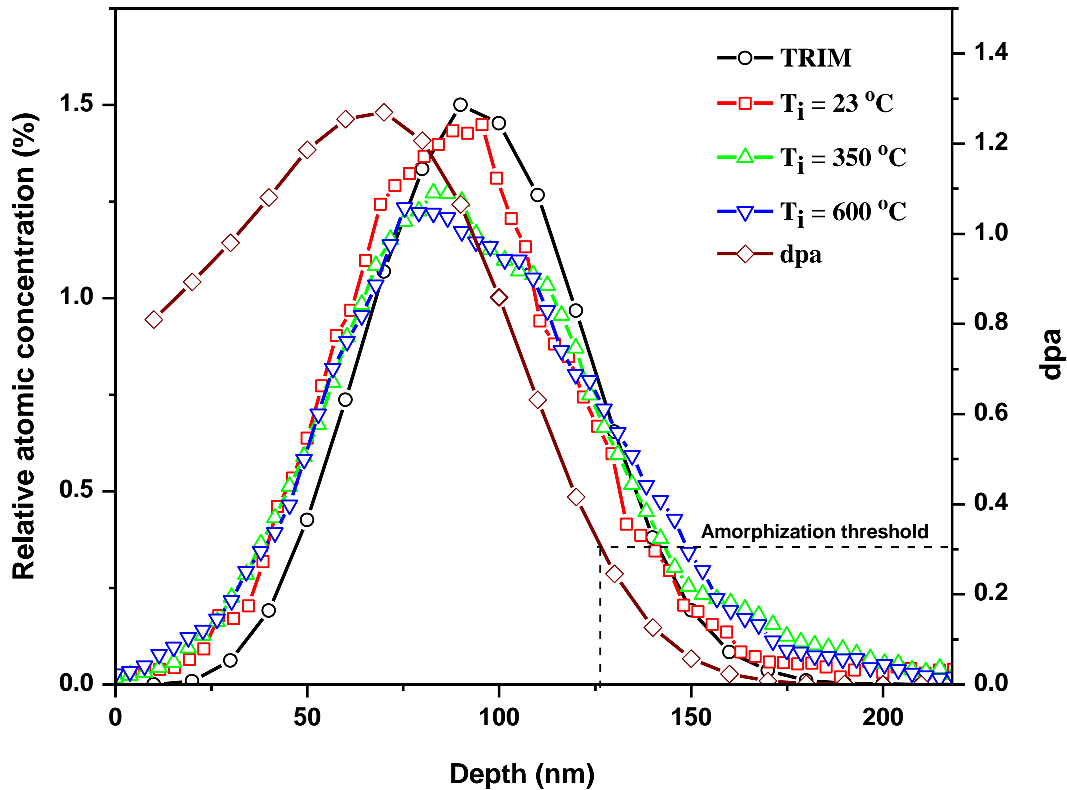

Fig. 1. The depth profiles of 200 keV Se implanted into SiC at room temperature, 350 °C and 600 °C from RBS, compared to SRIM 2012 simulated Se depth profile with the corresponding displacement per atom (dpa) (left scale).

Table 1. A comparison of the first four moments of the experimental and SRIM simulated profiles. The selenium experimental profiles of RT, 350 °C and 600 °C were fitted to the Edgeworth function.

Parameter	SRIM	RT	350 °C	600 °C
Projected ranges (Rp) (nm)	89.6	87.7 ± 2.9	89.9 ± 2.9	90.8 ± 2.9
Straggling (ΔRp) (nm)	26.5	29.9 ± 2.9	34.0 ± 2.9	35.3 ± 2.9
Kurtosis (β)	2.78	2.97	2.95	2.9
Skewness (γ)	0.13	0.28	0.05	0.3

The radiation damage level in the substrates was evaluated in terms of the displacements per atom (dpa). At room temperature, amorphization of SiC occurs in regions with damage levels greater than 0.3 dpa [16] [17]. This is corresponding to a depth of approximately 125 nm from the surface. This clearly indicates that implantation at RT produced amorphization in about 70% of the implanted thickness. Fig. 1 also shows that the maximum damage of 1.3 dpa occurred at a depth of about 70 nm, which is considerably lower than the projected range. For the hot implantation (350°C and 600°C), the complete amorphization cannot be achieved. This is because the implantation temperature was above the critical amorphization temperature of SiC [5].

The RBS depth profiles before and after isochronal annealing at temperatures ranging from 1000 to 1500 °C in steps of 100 °C for 10 hours are shown in Fig. 2. In all implanted samples shown in Fig. 2, no change was observed in the peak position of the Se profile after annealing from 1000 up to 1200 °C. This indicates the lack of measurable shift at these temperatures. A peak shift towards the surface began after the annealing at 1300 ° C and progressed with annealing at higher annealing temperatures as can be seen in Fig. 3, suggesting that SiC had been removed by thermal etching. The molecules on high-energy surfaces sublimated into the vacuum, resulting in a reduction in the total energy of the system, thereby leading to roughening the sample surface [18]. Evidence of the thermal etching was confirmed by SEM measurements discussed later in the paper. The annealing at 1500 °C caused the decomposition of silicon carbide for the sample implanted at room temperature. This is clearly shown by the formation of a carbon layer at the sample's surface - see Fig.4.

The retention ratio of selenium during heat treatment is depicted in Fig. 5. A loss of some of the Se from all the implanted samples was observed after annealing at 1300 °C (about 10 %). This loss became more significant with increasing temperature in the case of the sample implanted at RT, while no further loss is noticeable for those implanted at 350 °C and 600 °C. This behaviour is correlated with pores on the sample surface at high annealing temperature, as will be discussed later in SEM measurements - appreciable at the RT implanted sample - which acts as pathways for the release of the implanted Se atoms into the vacuum upon arrival to the surface, because its boiling point (685°C) is significantly less than the annealing temperatures. It is also due to the profile shift toward the surface at these temperatures.

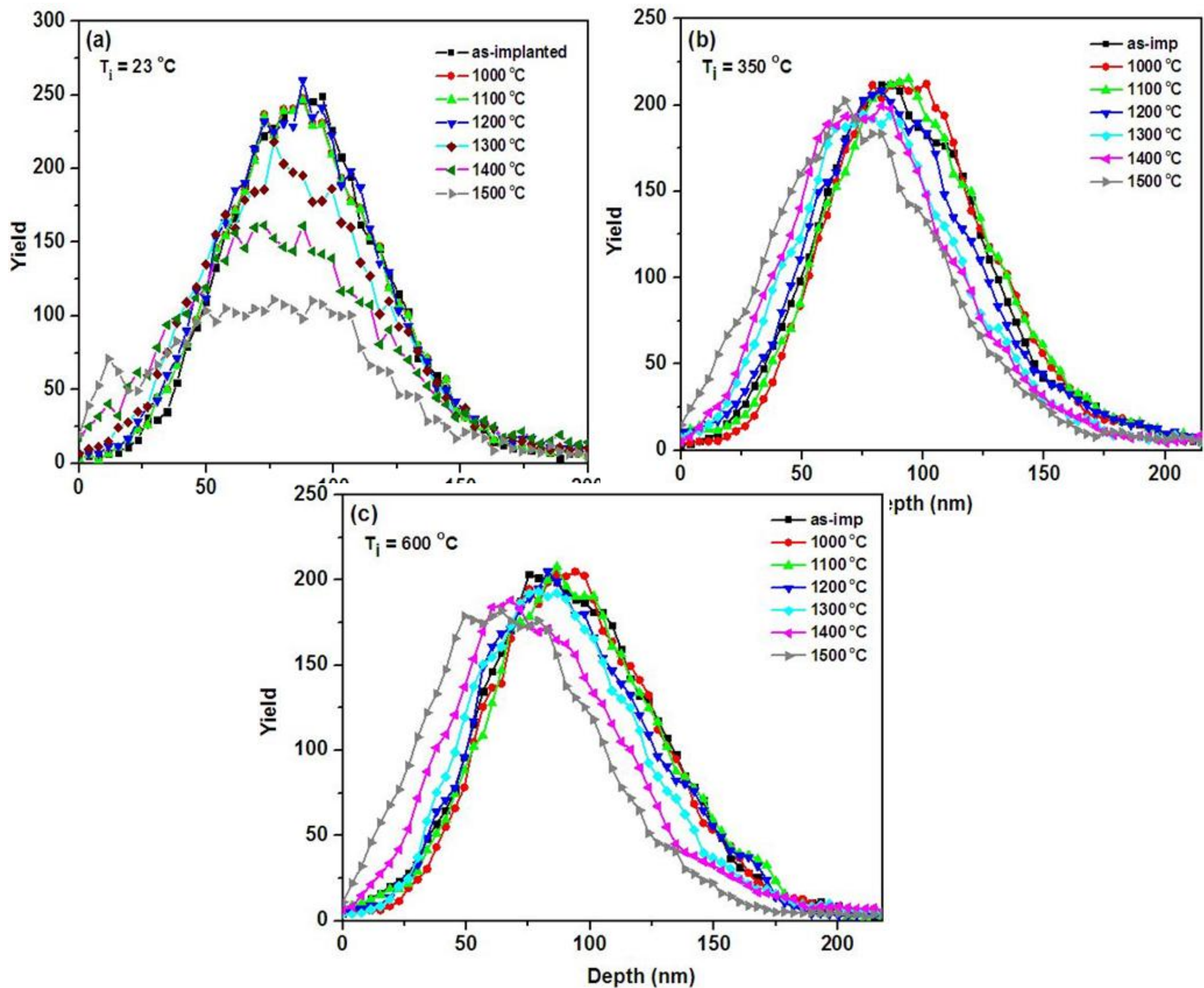

Fig.2. Depth profiles of selenium implanted in 3C–SiC at (a) room temperature, (b) 350 °C and (c) 600 °C after sequential isochronal annealing from 1000 to 1500 °C for 10 hours.

The broadening of the implanted Se profile in SiC was quantified by the full width at half maximum (FWHM) of the peaks. The FWHM values were obtained from the range straggling (ΔRp) by: $\mathrm{FWHM} = 2\Delta\mathrm{Rp}\sqrt{2\ln 2}$ after fitting the profiles to a Gaussian function. Fig. 6 shows the square of FWHM values as a function of annealing temperature. No broadening occurred in the hot implanted samples (350 °C and 600 °C) after heat treatment in the temperature range 1000 to 1500 °C. For the sample implanted at room temperature, the FWHM of the Se profile remained nearly constant after annealing from 1000 up to 1200 °C. The width broadening became noticeable after annealing at 1300 °C. However, the increase in the FWHM is within the experimental error of the RBS depth scale. The peak has broadened significantly after annealing at 1400 °C and 1500°C. There are two possible reasons for this broadening, namely the diffusion of Selenium and the effects due to the increase of surface roughness (discussed in the SEM results).

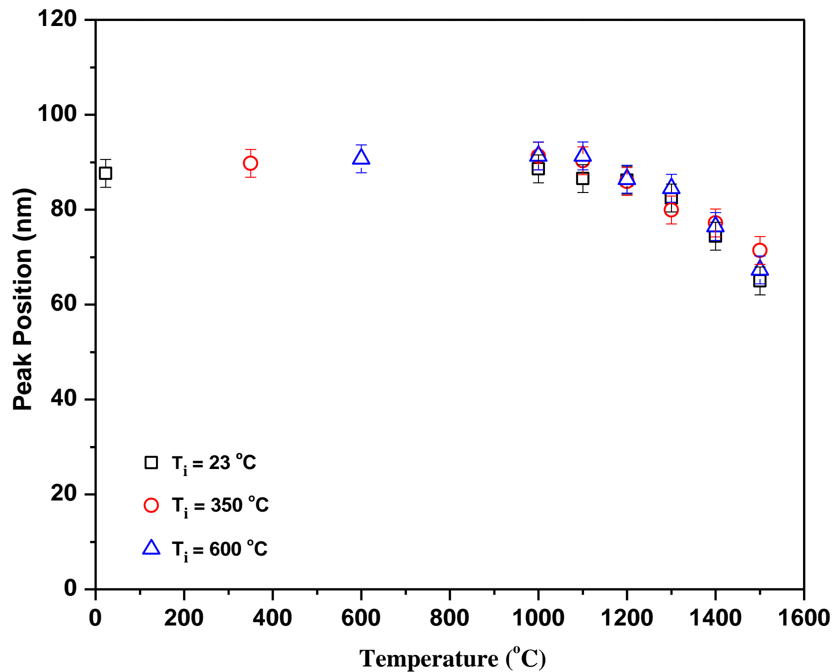

Fig.3. The peak position of implanted Se profile as a function of annealing temperature.

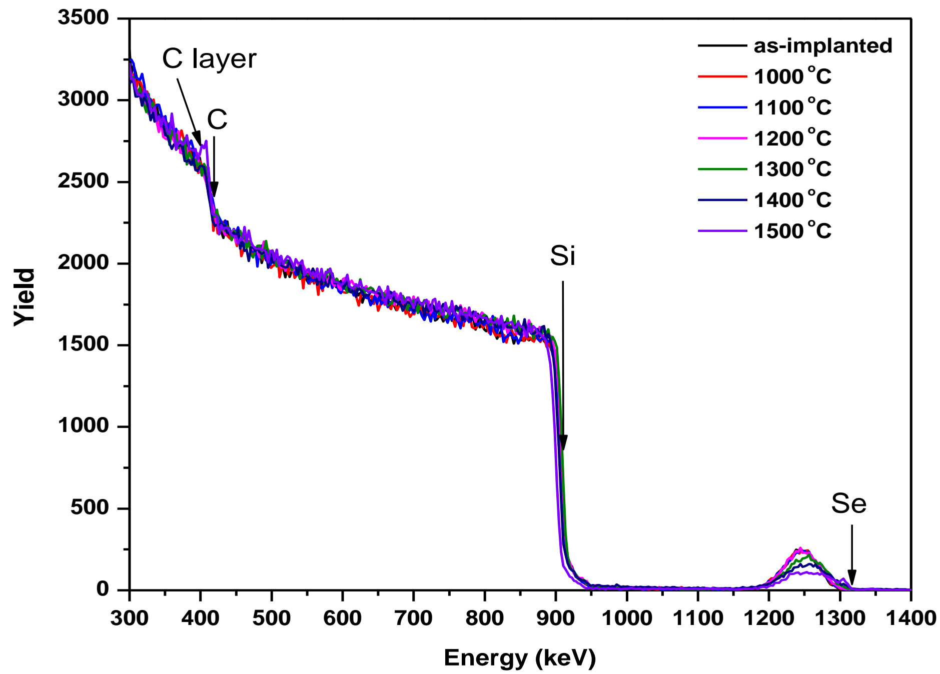

Fig.4. RBS spectra of selenium implanted in 3C–SiC at room temperature and after isochronal annealing from 1000 to 1500 °C for 10 hours. Arrows indicate the surface positions of elements.

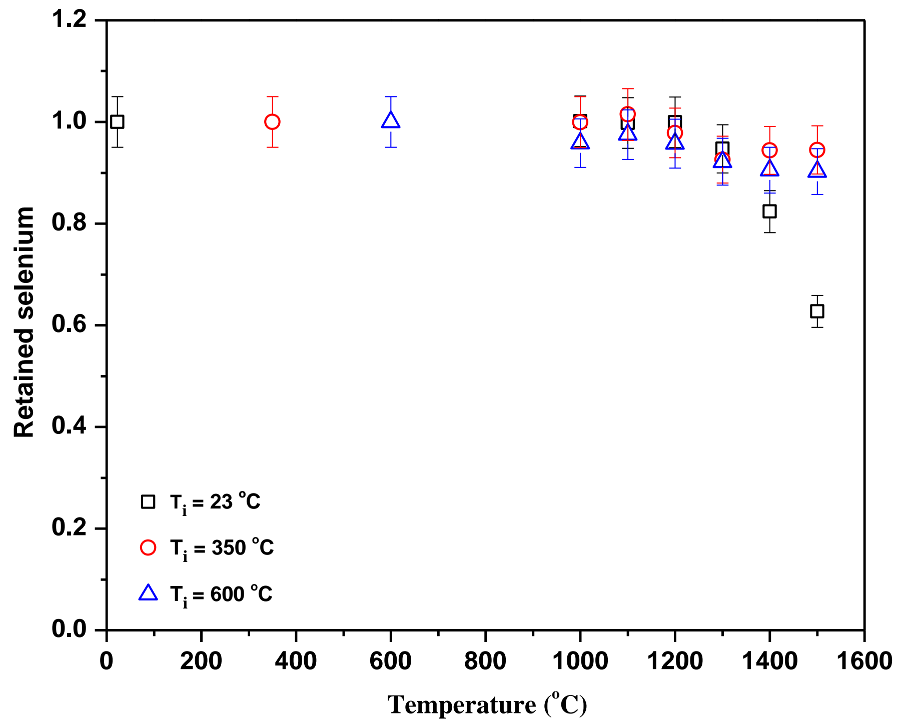

Fig.5. The retained ratio of Se implanted into polycrystalline SiC profiles as a function of annealing temperature.

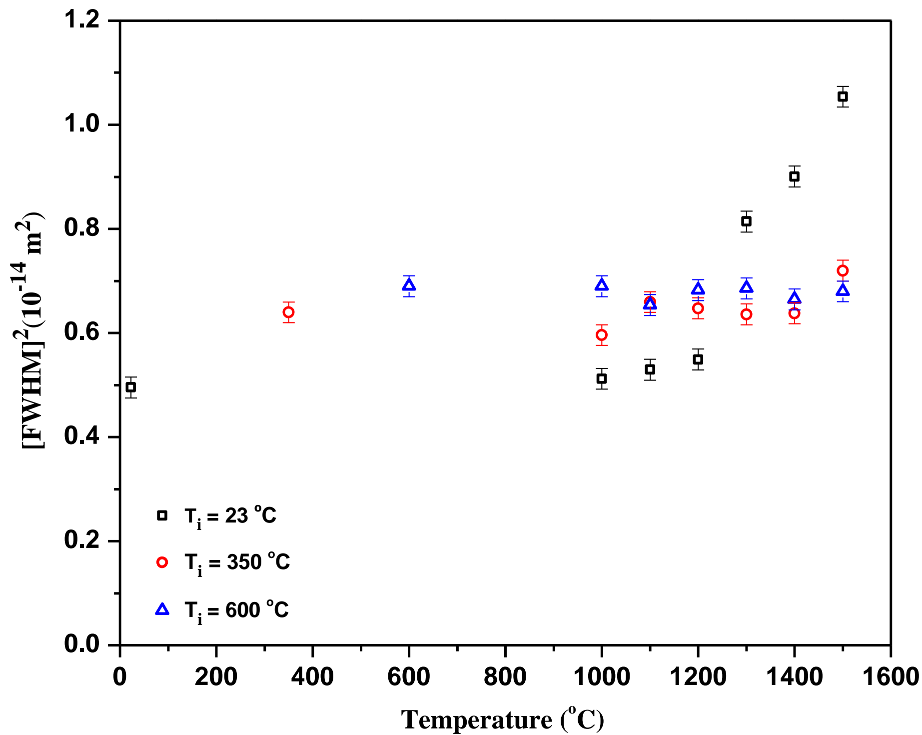

Fig.6. The square of the full width at half maximum of implanted Se profiles as a function of annealing temperature.

The effects of implantation and annealing temperature on the surface morphology were investigated using Scanning Electron Microscopy (SEM). Fig.7 shows the SEM images of polycrystalline SiC surfaces before and after implantation at RT, 350 °C and 600 °C.

The pristine surface showed some polishing marks because of the mechanical polishing process as shown in Fig. 7(a). After implantation at RT, the surface became flat and featureless (Fig. 6(b)). This is due to sputtering of the surface atoms induced by bombarding them with energetic particles, and the swelling in the amorphous layer [19]. Implantation at 350 °C (near to the critical temperature for amorphization) led to reducing the polishing marks, but the grains were still visible (Fig. 7(c)), indicating the presence of the crystalline structure. No significant change was observed on the surface of the sample implanted at 600 °C compared to that one of the pristine (Fig. 6(d)), because the implantation was performed at a temperature well above the critical temperature for amorphization.

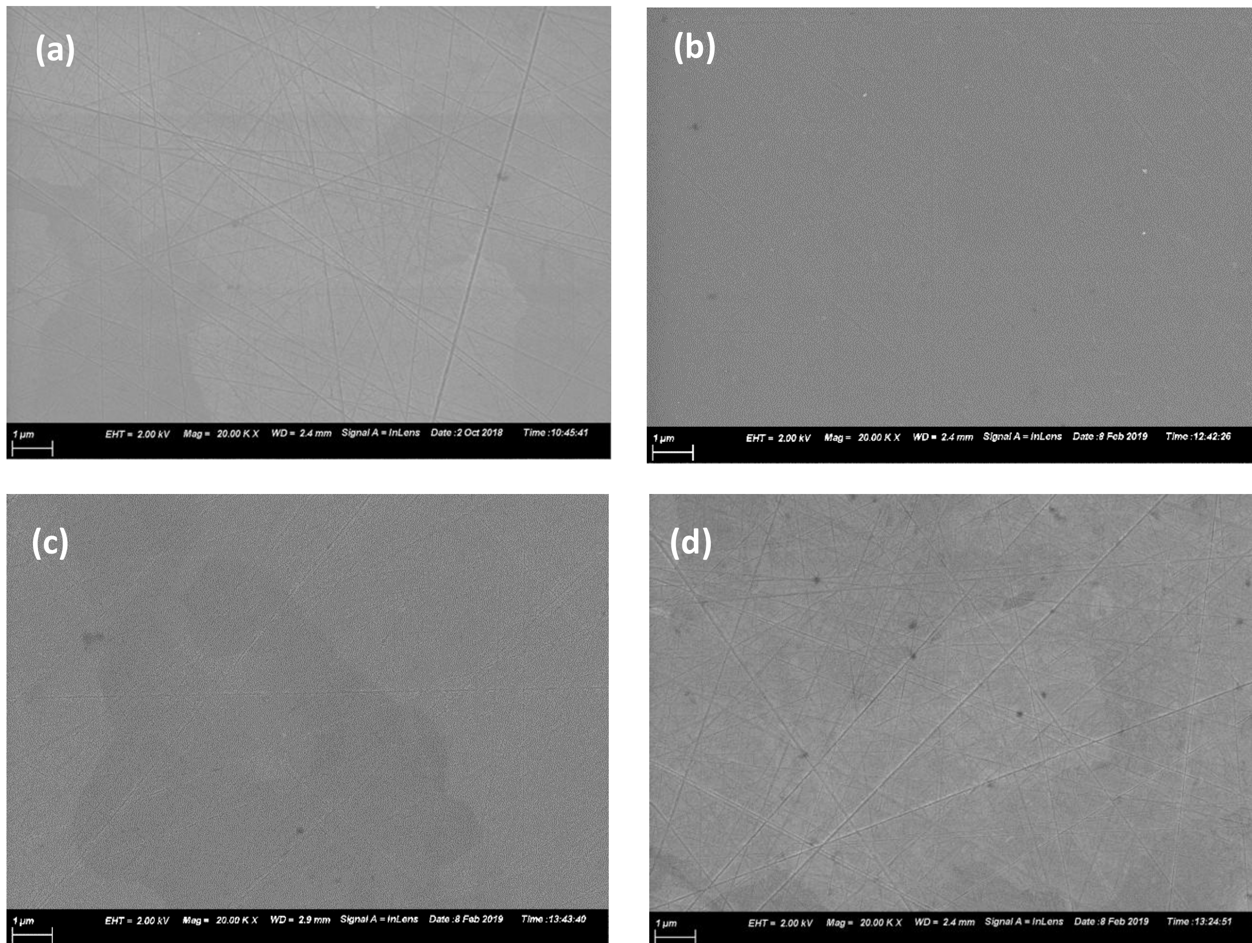

Fig. 7. SEM images of (a) Pristine poly-SiC, and after implantation with Se at (b) RT, (c) 350 °C and (d) 600 °C.

The surface of the RT implanted sample after annealing at 1000 °C was still featureless (not shown), it is similar to that in Fig. 7(b). At 1100 °C, crystallites were clearly visible on the surface - see Fig. 8(a). As can be seen in Fig. 8(b), the crystals grew in size and became more apparent with increasing temperature. Annealing at 1400 °C and 1500 °C led to the formation of large crystals with fewer pores - see Fig.8(c). Fig. 8 also shows that after annealing at 1300 ^{o} C, the surface became rough and continues to increase at higher annealing temperatures. This may confirm the broadening of the RBS depth profile of selenium at these temperatures due to rough surfaces of samples.

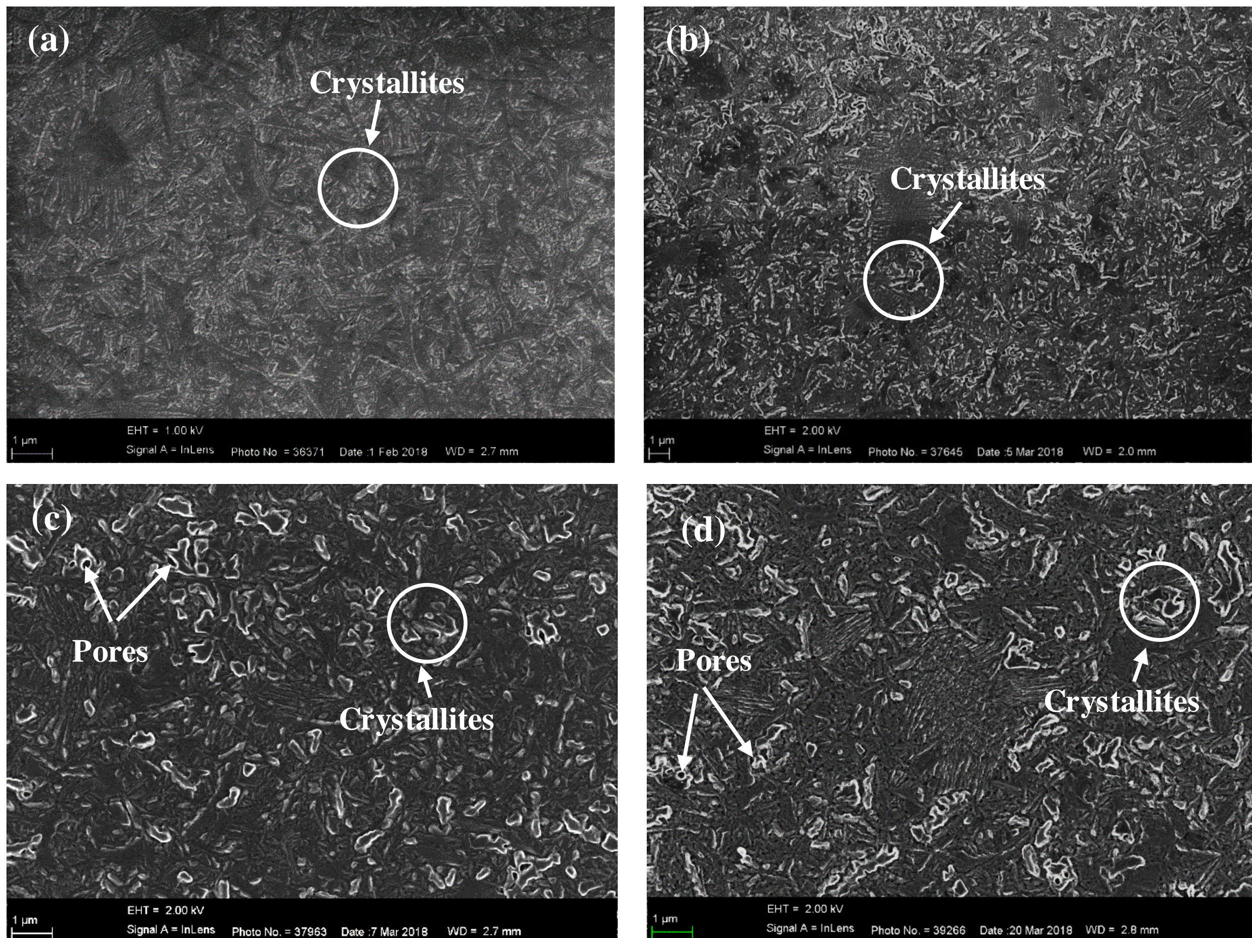

Fig. 8. SEM images of the RT implanted sample after vacuum annealing at (a) 1100 °C, (b) 1300 °C, (c) 1400°C and (d) 1500°C for 10 hours.

Fig. 9(a and b), showed that the grains and their boundaries are clearly visible and the polishing marks still remained on the surfaces after annealing at 1100 °C and 1200°C (not shown) for both samples implanted at 350 and 600 °C. In the case of the 350 °C implanted sample, annealing at 1300 °C and above, the grain boundaries became more apparent, as well as the presence of pore openings on these boundaries as shown in Fig. 10(a and b). These observations are due to thermal etching and uneven grain growth, which occurred during annealing. The low surface bonding energies at and near grain boundaries have made their SiC molecules sublimate faster than those in the middle of crystal surfaces [18].

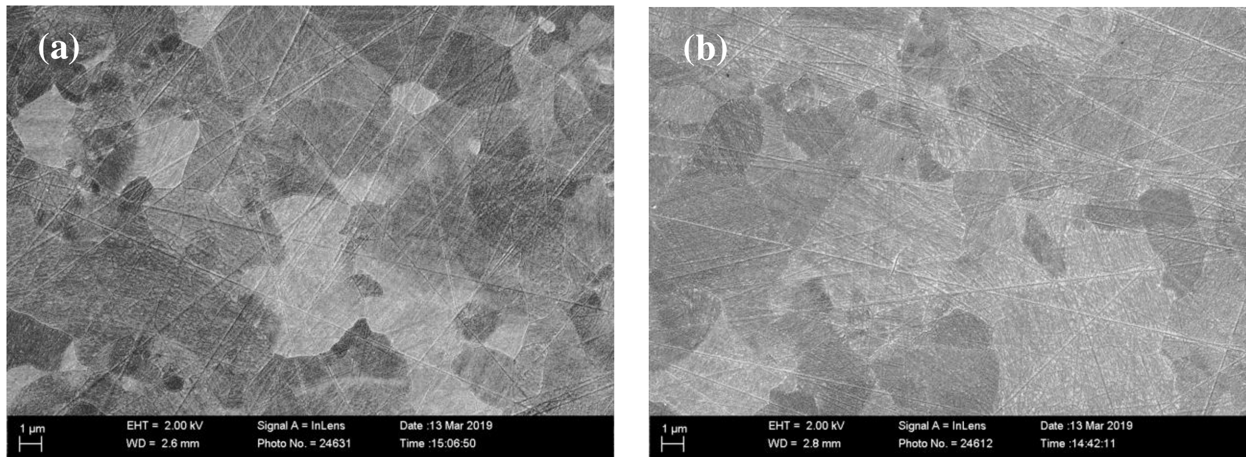

Fig. 9. SEM images after vacuum annealing at 1100 °C for samples implanted at (a) 350 °C and (b) 600°C for 10 hours.

In contrast to 350 °C implanted sample, the surface pores are not observed in the sample implanted at 600 °C after annealing at 1300 °C-see Fig. 10(c), whereas annealing at 1400 and 1500 °C led to the appearance of surface pores, as well as a significant reduction in the visibility and number of polishing marks.

An inspection of the SEM images shows a decrease in the grain sizes of the implanted samples after annealing and with increasing temperature. The Se ion bombardment introduced many defects in the crystalline 3C-SiC. Some of these defects are line and plane defects. Stacking faults introduce either new SiC poly-types or smaller 6H-SiC crystallites. The implanted Se impurities also inhibit crystal growth leading to smaller crystallites with increasing annealing temperature.

Furthermore, the appearance of pore openings on surfaces of the hot implanted samples at higher annealing temperatures as can be seen in Fig. 10. In contrast, these openings cannot be observed in the case of the RT implanted sample (see Fig. 8). This might be due to the significant change in stress/strain in the hot implanted samples at these temperatures (discussed in the Raman analysis).

The first-order Raman spectra of the pristine sample and as-implanted at RT, 350 °C and 600 °C samples are shown in Fig. 11. The spectrum of the pristine sample displays three features in the 700-1100 cm^{-1} range, indicating the characteristic Raman modes of silicon carbide [20][21][22].The two peaks at 771 and 797 cm^{-1} correspond to the transverse optic (TO) mode,

and the peak at 966.5 cm^{-1} correspond to longitudinal optic (LO) mode. As can be seen from the Fig. 11, implantation at room temperature resulted in the disappearance of the characteristic SiC Raman peaks, indicating that the SiC layer is amorphized. The three dominant features of Raman spectra of SiC between 700 and 1100 cm^{-1} were retained after implanted it at 350 °C and/ or 600 °C.

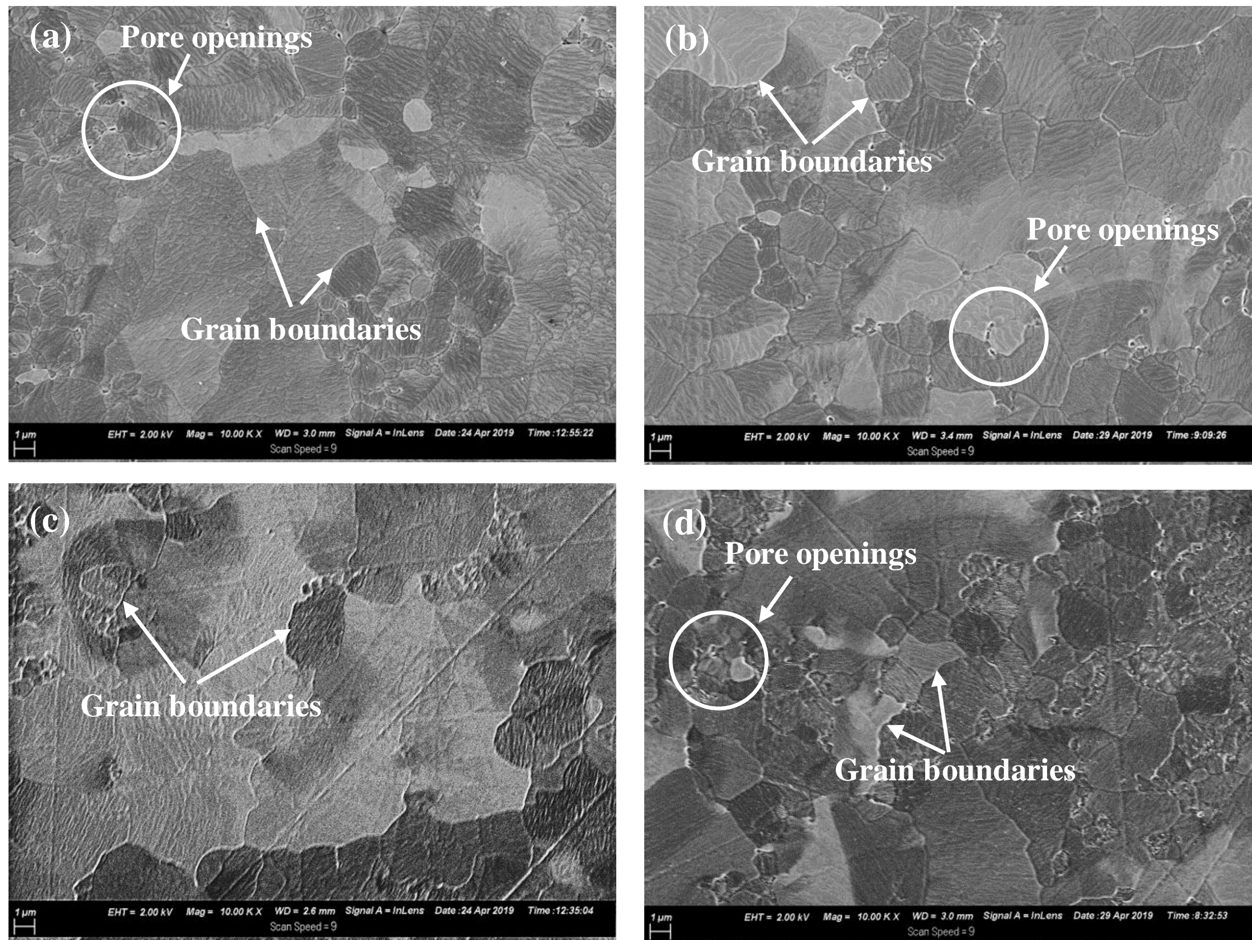

Fig. 10. SEM images of the 350 °C implanted sample after vacuum annealing at (a) 1300 °C, (b) 1400 °C, the 600 °C implanted sample after vacuum annealing at (c) 1300 °C and (d) 1400 °C for 10 hours..

Fig. 11 also shows that the Raman intensity of samples implanted at 600 °C is higher compared to those of 350 °C, suggesting a lower concentration of defects in the former [21].

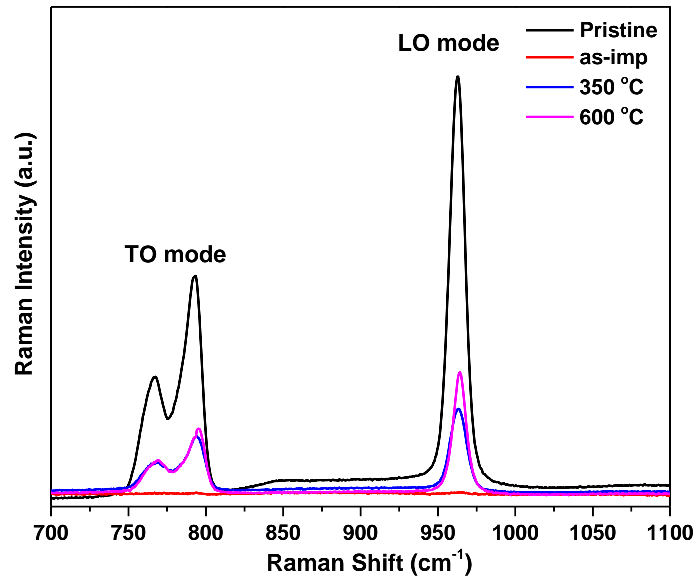

Fig. 11. First order Raman spectra of the pristine poly-SiC and after implantation with Se at RT, 350 °C and 600 °C.

Annealing of the RT implanted sample at 1000 °C led to the reappearance of the characteristic spectrum of SiC with the main peaks (similar to those obtained from the pristine sample) as shown in Fig. 12, clearly indicating the recrystallization of SiC. The lower intensity of the peaks compared with those of the pristine sample suggests the presence of remaining defects in the recrystallized SiC layer.

The average stress in the samples was calculated using the change in LO Raman mode as discussed in [23]. Fig. 13 shows the evolution of residual stress with annealing temperature in SiC substrates. Implantation at 350 ºC caused a modification in the mechanical properties of the sample with a residual tensile stress of 0.86 GPa. This is due to the increase of the chemical bond lengths, relative to their lengths in the unstressed crystals [24] [25]. Annealing at 1000 °C showed the similar stress level. No change in the residual stress was observed after annealing at 1100 °C. Annealing at 1200 °C and 1300 °C reduced the amount of residual tensile stresses to the same level. Further annealing after 1400 ° C, the tensile stress began to decrease, reaching its minimum value of 0.75 GPa at 1500 °C. For the sample implanted at 600 °C, the implantation induced tensile stress of 0.95 GPa After annealing in the range between 1000 °C and 1500 °C, approximately the same scenario was

repeated, which occurred as in the sample grown at 350 °C. This indicates that the internal stress distributions are almost the same. In this study, the residual stress in the as-implanted sample cannot be calculated in the case of room temperature. Because of the disappearance of Raman mode due to the amorphization. Whereas, Fig. 13 shows that the residual tensile stress was 0.94 GPa after annealing at 1000 °C. Annealing at 1100 °C, the tensile stress decreased to 0.39 GPa. Annealing at 1200 °C resulted in increased tensile stress again where it became equal to those implanted in hot temperatures. Further annealing, no significant change in residual stress occurred with increasing temperature. Strange behaviour at 1100 °C can be attributed to the increase in the density of stacking faults at this temperature, and thus increasing the structural disorder within SiC. Consequently, Raman peak positions are shifted to higher wavenumbers indicating less tensile stress [26]. Comparing these results with the Se migration results in SiC discussed earlier (especially at 1100 °C), the difference in residual stress level has no role in migration of implanted Se.

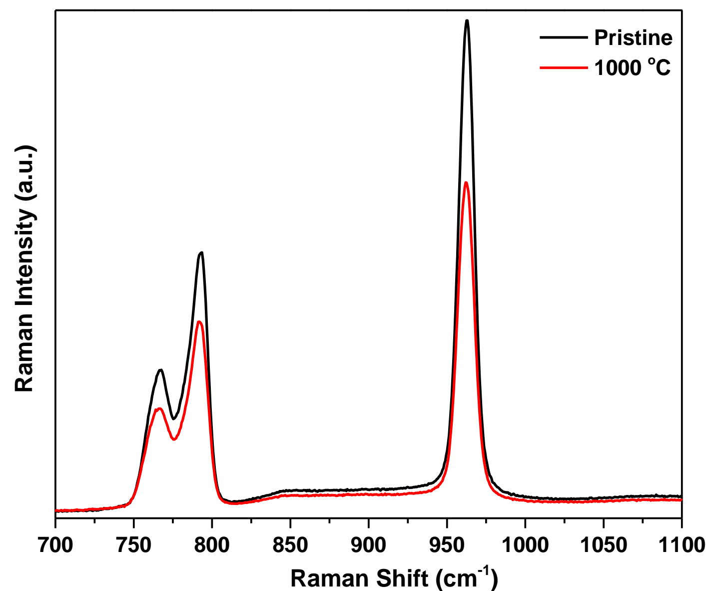

Fig. 12. First order Raman spectra of the pristine poly-SiC compared with the RT implanted sample after vacuum annealing at 1000 °C.

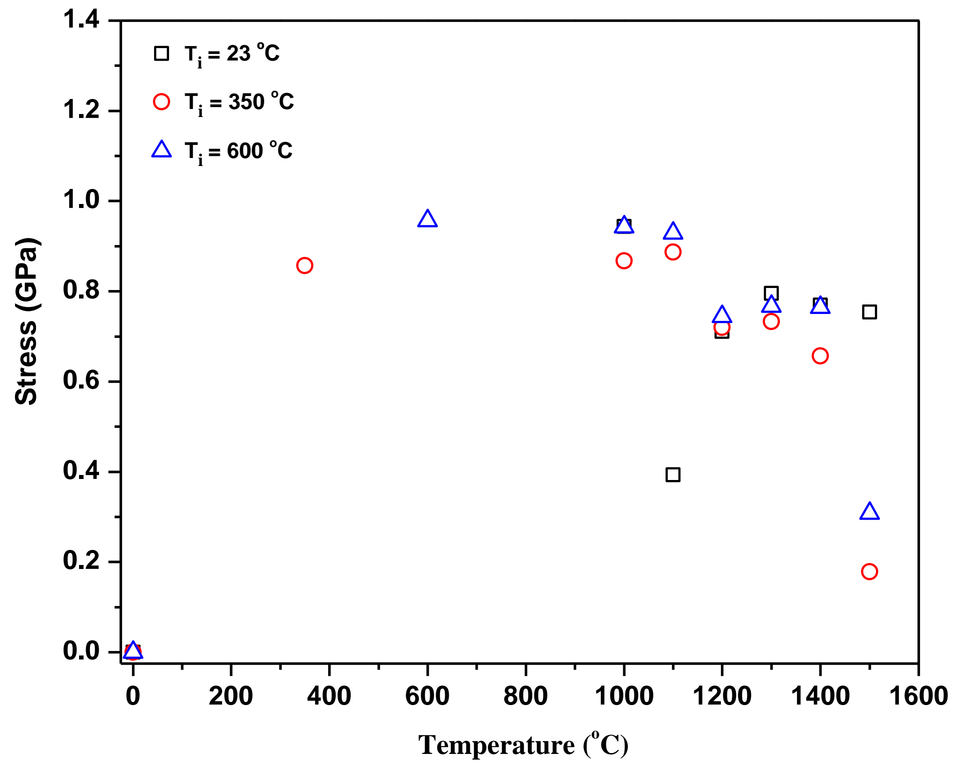

Fig. 13. The residual stress in the poly-SiC samples implanted with Se at RT, 350 °C and 600 °C as a function of annealing temperature.

4. CONCLUSION

The effect of heat treatment on the migration behaviour of Se in polycrystalline SiC was investigated. The RBS depth profile obtained from the RT as-implanted sample showed that the majority of implanted Se is embedded in the bombardment-induced amorphous layer, and broadening of the implanted Se profile began after annealing at 1300°C. No broadening of the implanted Se profile has been observed in the samples implanted at hot temperatures (350°C and 600°C) during annealing up to 1500 °C. Thermal etching occurred after annealing at 1300 ° C and increased with annealing temperature, resulting in a shift of the Se profiles toward the surface. In all cases, the shift was accompanied by a loss of about 10 % of Se ions after annealing at beginning of thermal etching. This loss became more significant with increasing thermal etching in the case of the RT implanted sample, while no further loss was noticeable for those implanted at 350 °C and 600 °C. SEM results showed that the topography before and after annealing depends on the substrate temperature of implantation. Raman results showed that implantation at RT led to an amorphization of the near-surface of the SiC layer. The samples implanted above the critical amorphization temperature and under the same bombardment conditions as cold implant, retained their crystalline structure with some radiation damage. It also showed that annealing temperature has a significant effect on the recovery of the crystal structure of SiC, as well as the presence of tensile stress inside the substrates. Residual stress plays no role in the migration of implanted Se.

ACKNOWLEDGEMENT

Financial support by the National Research Foundation and The World Academy of Science is gratefully acknowledged.

REFERENCES

[1] Pebble Bed Modular Reactor, International Atomic Energy Agency, *Vienna, Austria, report 70, August 2011.*

[2] J. B. Malherbe, E. Friedland, N. G. Van Der Berg, "Ion beam analysis of materials in the PBMR reactor." *Nuclear Instruments and Methods in Physics Research Section B: Beam Interactions with Materials and Atoms, vol. 266, no. 8, pp. 1373-1377, 2008.*

[3] O. Ö. Gülol, Ü. Çolak, and B. Yıldırım. "Performance analysis of TRISO coated fuel particles with kernel migration." *Journal of Nuclear Materials, vol. 374, no. 1-2, pp .168-177, 2008.*

[4] W. F. Skerjanc, J. T. Maki, B. P. Collin, D. A. Petti "Evaluation of design parameters for TRISO-coated fuel particles to establish manufacturing critical limits using PARFUME." *Journal of Nuclear Materials, vol. 469, pp. 99-105, 2016.*

[5] J. B. Malherbe, "Diffusion of fission products and radiation damage in SiC," *J. Phys. D. Appl. Phys.*, vol. 46, no. 47, pp. 1–52, 2013.

[6] N.G. van der Berg, J.B. Malherbe, A.J. Botha, E. Friedland, "SEM Analysis of the Microstructure of the Layers in Triple Coated Isotropic (TRISO) Particles." *Surf. Interface Anal, vol. 42, no. 6-7, pp. 1156 -1159, 2010.*

[7] L. L Snead, T. Nozawa, Y. Katoh, T. S. Byun, S. Kondo and D. A. Petti, "Handbook of SiC properties for fuel performance modeling." *Journal of nuclear materials, vol. 371, no. 1-3, pp. 329-377, 2007.*

[8] P. Hosemanna, J.N. Martos, D. Frazer, G. Vasudevamurthy, T.S. Byun, J.D. Hunn, B.C. Jolly, K. Terrani, M. Okuniewski "Mechanical characteristics of SiC coating layer in TRISO fuel particles." *Journal of Nuclear Materials, vol. 442, no. 1-3, pp. 133-142, 2013.*

[9] American Elements, accessed March 09, 2019, Selenium *www.americanele- ments.com.*

[10] Z.A.Y. Abdalla, M.Y.A. Ismail, E.G. Njoroge, T.T. Hlatshwayo, E. Wendler, J.B. Malherbe, Migration behaviour of selenium implanted into polycrystalline 3C-SiC, *Vacuum 175 (2020) 109235.*

[11] E. Friedland, J.B. Malherbe, N.G. van der Berg, T. Hlatshwayo, A.J. Botha, E. Wendler, W. Wesch, "Study of silver diffusion in silicon carbide," *J. Nucl. Mater.*, vol. 389, no. 2, pp. 326–331, 2009.

[12] K. Gärtner,"Modified master equation approach of axial dechanneling in perfect

compound crystals”, *Nuclear Instruments and Methods in Physics Research Section B: Beam Interactions with Materials and Atoms 227, no. 4 (2005): 522-530.*

[13] J. B. Malherbe, P. A. Selyshchev, O. S. Odutemowo, C. C. Theron, E. G. Njoroge, D. F. Langa and T. T. Hlatshwayo, “Diffusion of a mono-energetic implanted species with a Gaussian profile,” *Nucl. Instruments Methods Phys. Res. Sect. B Beam Interact. with Mater. Atoms*, vol. 406, pp. 708–713, Sep. 2017.

[14] R. Devanathan, W. J. Weber, and F. Gao, “Atomic scale simulation of defect production in irradiated 3C-SiC,” *J. Appl. Phys.*, vol. 90, no. 5, pp. 2303–2309, 2001.

[15] X. F. Qin, S. Li, F.X. Wang, and Y. Liang. "The mean projected range and range straggling of Nd ions implanted in silicon carbide." *In Key Engineering Materials, vol. 474, pp. 565-569. Trans Tech Publications Ltd, 2011.*

[16] C. J. McHargue, J. M. Williams, "Ion implantation effects in silicon carbide." Nuclear Instruments and Methods in Physics Research Section B: Beam Interactions with Materials and Atoms, vol. 80, pp. 889-894, 1993.

[17] Xu. Wang, Li. Junhan, Jie Wang, Jie Song, Fuqiang Zhao, Hexi Tang, Bing-sheng Li, and An-Li Xiong, "Microstructure investigation of damage recovery in SiC by swift heavy ion irradiation." *Material Design & Processing Communications, vol. 1, no. 5, e87, 2019.*

[18] N.G. van der Berg, J.B. Malherbe, A.J. Botha and E. Friedland, “Thermal etching of SiC,” *Appl. Surf. Sci, vol. 258, pp. 5561 -5566, 2012.*

[19] J. B. Malherbe, N. G van der Berg, R. J. Kuhudzai, T. T. Hlatshwayo, T. T. Thabethe, O. S. Odutemowo, C. C. Theron, E. Friedland, A. J. Botha, E. Wendler, “Scanning electron microscopy of the surfaces of ion implanted SiC,” *Nuclear Instruments and Methods in Physics Research Section B: Beam Interactions with Materials and Atoms, vol. 354, pp. 23-27, 2015.*

[20] A. Deslandes, M. C. Guenette, L. Thomsen, M. Ionescu, I. Karatchevtseva, and G. R. Lumpkin, “Retention and damage in 3C- b SiC irradiated with He and H ions,” *J. Nucl. Mater.*, vol. 469, pp. 187–193, 2016.

[21] S. Nakashima and H. Harima, “Raman Investigation of SiC Polytypes,” *phys. stat. sol.*, vol. 162, pp. 39–64, 1997.

[22] S. Sorieul, J. M Costantini, L. Gosmain, L. Thomé, J. J. Grob, "Raman spectroscopy study of heavy-ion-irradiated α-SiC." *Journal of Physics: Condensed Matter, vol. 18, no.*

22, pp. 5235, 2006.

[23] Z. Xu, Z. He, Y. Song, X. Fu, M. Rommel, X. Luo, A. Hartmaier, J. Zhang and F. Fang, "Topic review: application of Raman spectroscopy characterization in micro/nano-machining." *Micromachines 9, no. 7 (2018): 361.*

[24] D. Tuschel, "Stress, Strain, and Raman Spectroscopy," *Spectroscopy, vol. 34, no. 9, pp. 10-22, 2019.*

[25] E. Wendler, T. Bierschenk, F Felgenträger, J.Sommerfeld, W. Wesch, D. Alber, G. Bukalis, L. C. Prinsloo, N. Van der Berg, E. Friedland and J. B. Malherbe, "Damage formation and optical absorption in neutron irradiated SiC," *Nucl. Inst. Methods Phys. Res. B*, vol. 286, pp. 97–101, 2012.

[26] H. Jin, S. Yoshida, L. Lamberti, and M. T. Lin," *Advancement of Optical Methods in Experimental Mechanics, Volume 3", Proceedings of the 2015 Annual Conference on Experimental and Applied Mechanics, Springer, 2015.*